

The effect of high temperatures on the electrical characteristics of Au/n-GaAs Schottky diodes

S.M. Tunhuma, F.D. Auret, M.J. Legodi, M. Diale*

Physics department, University of Pretoria, Pretoria 0002, South Africa

ARTICLE INFO

Article history:

Received 15 May 2015

Received in revised form

6 August 2015

Accepted 7 August 2015

Available online 8 August 2015

Keywords:

Barrier height

Annealing

DLTS

GaAs

EL2 defect

ABSTRACT

In this study, the current–voltage (I – V) and capacitance–voltage (C – V) characteristics of Au/n-GaAs Schottky diodes have been measured over a wide temperature range, 80–480 K. The diodes were rectifying throughout the range and showed good thermal stability. Room temperature values for the ideality factor, I – V barrier height and C – V barrier height were found to be $n=1.10$, $\phi_{IV}=0.85$ eV and $\phi_{CV}=0.96$ eV, respectively. ϕ_{IV} increases and n decreases with an increase in temperature. We investigated the effect of elevated temperatures on the barrier height and ideality factor by measuring the diodes at a high temperature (annealing mode) then immediately afterwards measuring at room temperature (post annealing mode). The measurements indicate I – V characteristics that degrade permanently above 300 K. Permanent changes to the C – V characteristics were observed only above 400 K. We also noted a discrepancy in the C – V barrier height and carrier concentration between 340 and 400 K, which we attribute to the influence of the EL2 defect (positioned 0.83 eV below the conduction band minima) on the free carrier density. Consequently, we were able to fit the ϕ_{CV} versus temperature curve into two regions with temperature coefficients -6.9×10^{-4} eV/K and -2.2×10^{-4} eV/K above and below 400 K.

© 2015 Elsevier B.V. All rights reserved.

1. Introduction

Gallium Arsenide is a very important direct bandgap semiconductor. At present it is used for many applications such as solar cells in space, sources and detectors in optical fibres and as microwave sources [1–3]. The high electron mobility and high carrier saturation velocity of the material makes it ideally suited for the fabrication of high frequency and low power devices [4]. Several opto-electronic devices have been implemented on it to date. These include multi junction photovoltaics, MOSFETs and low noise avalanche photodiodes [5,6]. More often these devices require metallization, therefore in order to understand their electrical characteristics we use the simple metal semiconductor (MS) structure also known as the Schottky barrier diode [4].

The quality of a Schottky contact is notably determined by the quality of the interface between the deposited metal and the semiconductor surface [7]. In GaAs-based devices the performance has been experimentally shown to be affected to a greater extent by surface and interface defect density and also the series resistance [8]. According to Tung [9,10] it can also be explained in the chemical bonding picture, where the diode characteristics

depend on the atomic structure of the MS interface.

Several researchers have studied the electrical characteristics of Au/n-GaAs Schottky diodes and have reported a strong dependence of diode characteristics on temperature [4,7,8,11–13]. Kim et al. [14] studied the temperature dependence of Au/n-GaAs I – V characteristics using a semi analytical model in the 83–323 K temperature range. They reported that the variations in the characteristics with temperature were consistent with those of the energy band gap. Örzeli et al. [12] explained the temperature dependence of the I – V and C – V characteristics at high temperatures (280–415 K) of Au/n-GaAs Schottky diodes using a Gaussian distribution of the Schottky barrier height. Similar experiments have been undertaken with samples exposed to and measured at the same high temperatures in other materials [15,16]. It is also important to take note of any changes and modifications as they occur when the device is exposed to high temperatures during measurement or operation since diode electrical characteristics are sensitive to heat treatment [17]. The annealing behaviour of GaAs Schottky diodes has already been the subject of a number of investigations [18–21]. Changes brought about to the diode characteristics by thermal annealing have variously been attributed to solid-phase reactions, dispersion of native oxides and failure of diffusion barriers at the interface [21,22].

However, most of these annealing studies were done systematically by exposing the diodes to high temperatures and then

* Corresponding author.

E-mail address: mmantsae.diale@up.ac.za (M. Diale).

measuring them at room temperature. There is a need to compare the measurements done during annealing and post annealing. This is because, as the temperature increases, the diodes are annealed and interfacial reactions may ensue. After exposure to these high temperatures the devices may be operated at a different, and usually lower, temperature. Studying the behaviour of the devices during annealing and post annealing may yield insights important for packaging, temperature processing and safe temperature operating ranges for the GaAs devices.

In this study gold contacts were deposited on epitaxial n-GaAs. We investigated the effects of high temperatures by comparing the rectification properties and thermal stability of the MS contacts in two modes: during annealing and post annealing. The post annealing measurements were undertaken at 300 K. These 300 K measurements were designed to track any modification to the Au/GaAs system accompanying the annealing. We also considered and monitored the effects of the EL2 defect on the free carrier concentration and the rectification properties of our samples using Laplace deep-level transient spectroscopy (L-DLTS).

2. Experimental details

MOCVD grown n-GaAs with a free carrier density of $1.4 \times 10^{15} \text{ cm}^{-3}$ and $\langle 100 \rangle$ orientation, supplied by Epi Materials Limited, was used. The wafers were first degreased by boiling in trichloroethylene for 5 min then in isopropanol for 3 min. They were then etched in a fresh solution of $\text{H}_2\text{O}:\text{H}_2\text{O}_2:\text{NH}_4\text{OH}$ (100:1:3) for 60 s and rinsed in 18 MΩ cm deionised water. The second etching step involved removal of the native oxide layer by etching the samples in a fresh $\text{H}_2\text{O}:\text{HCl}$ (1:1), followed by a rinse in deionised water then blow drying in compressed nitrogen gas. Au-Ge (88%:12%) ohmic contacts were evaporated on the back of the wafer in an Edwards 304 resistive coating unit pumped down to 4×10^{-7} mbar. This was followed by thermal annealing at 450 °C for 3 min in flowing argon gas.

The wafers were cleaned again, repeating the degreasing, etching and oxide removal steps. This time, an ultrasonic bath was used instead of boiling. Immediately thereafter the samples were transferred into the vacuum system for Schottky metallization. Circular contacts of 0.6 mm diameter and 500 Å thickness were resistively deposited on the epitaxial layer. Temperature dependent I - V and C - V characteristics were recorded in the 80–480 K range using a JANIS closed-cycle liquid helium cryostat, an HP4140B pico-ammeter and an HP4192A LF Impedance meter. A Lakeshore 332 temperature controller with a sensitivity of ± 0.1 K was used to control the temperature.

The I - V and C - V investigations were carried out in two modes: (1) during annealing, conducted at some elevated temperature in the 80–480 K range in 20 K steps, and (2) post annealing measurements, conducted at 300 K after the annealing described in (1). Once the correct annealing temperature was established, a further 5 min was allowed for the system to establish equilibrium. All the C - V measurements were done at 1 MHz. Finally, Laplace deep-level transient spectroscopy (L-DLTS) measurements were carried out in a JANIS cryostat within the temperature range 80–480 K.

3. Results and discussion

Our post annealing data is limited to measurements done above 300 K as no significant changes were noted for thermal treatment below 300 K. Fig. 1 shows the semi-logarithmic plot of the forward bias I - V characteristics of the Au/n-GaAs diodes obtained in the 80–480 K range in the annealing mode. The diodes

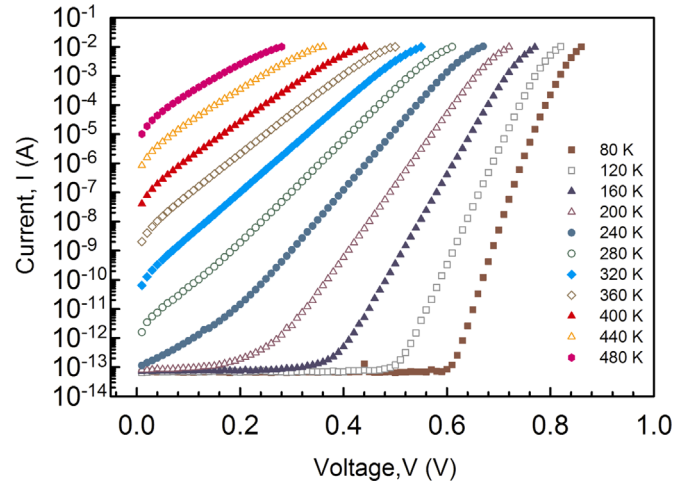


Fig. 1. Semi logarithmic forward current–voltage characteristics as a function of temperature for Au/n-GaAs Schottky diodes during annealing.

are rectifying throughout the temperature range indicating good thermal stability. The data in Fig. 1 was fitted satisfactorily in the linear regions of the curves using the pure thermionic emission model. No well-defined linear region is observed in the 400–480 K curves. These results differ with the post annealing mode forward bias characteristics which were all fitted satisfactorily using the thermionic emission theory up to 480 K.

For pure thermionic emission, and for $(V > 3kT/q)$ the relationship between the current I and the applied bias voltage V is given by:

$$I = AA^*T^2 \exp\left(-\frac{q\phi_0}{kT}\right) \left[\exp\left(\frac{q(V - IR_s)}{nkT}\right) - 1 \right] \quad (1)$$

where q is the electronic charge, k the Boltzmann constant, T the absolute temperature, R_s the series resistance, ϕ_0 ($=\phi_{IV}$) the zero-bias barrier height, A the diode area and A^* ($=8.16 \text{ A cm}^{-2} \text{ K}^{-2}$) is the Richardson's constant. The prefactor of the second exponential in Eq. (1) is the reverse saturation leakage current, I_s . The ideality factor n is given by [23]:

$$n = \frac{q}{kT} \left(\frac{dV}{d(\ln I)} \right) \quad (2)$$

n is a measure of adherence to the pure thermionic emission theory as it reflects barrier deformation under bias [11]. The zero bias barrier height, (ϕ_0) is obtained from the reverse saturation leakage current (I_s):

$$\phi_0 = \frac{kT}{q} \ln \frac{AA^*T^2}{I_s} \quad (3)$$

A plot of variation of n and ϕ_0 against temperature during annealing is shown in Fig. 2. ϕ_0 varies from 0.78 eV at 80 K to a maximum of 0.86 eV at 400 K where as n decreases from 1.21 at 80 K to 1.02 at 400 K. This behaviour of the barrier height during annealing is contrary to the negative temperature coefficient for n-GaAs and has been observed by other researchers [7,8,23,24]. The variation of diode characteristics confirms the linear correlation between n and ϕ_0 [25].

In both modes n and ϕ_0 show a strong dependence on temperature. The dependency on temperature of diode I - V characteristics has been accounted for as due to several factors, chief amongst them the local non-uniformities of the Schottky barrier. At high temperatures, there are possible inhomogeneities in the interface layer thickness and non-uniformities of the interfacial charges [26]. Other authors have attributed these to changes in

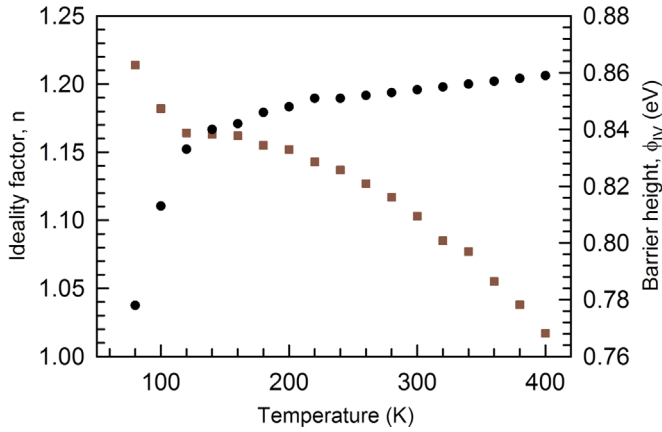


Fig. 2. I - V barrier height, ϕ_{IV} and ideality factor, n versus temperature for Au/n-GaAs Schottky diodes during annealing.

carrier transport mechanisms that is recombination-generation in the space charge region and tunnelling in the barrier [10,27,28]. The variation of ϕ_0 with temperature has also been linked to changes in the band gap [14].

Post annealing, n varies from 1.10 after 300 K to 1.14 after 480 K and ϕ_0 decreases from 0.85 eV to 0.79 eV in the same temperature range. Fig. 3 is a comparison between n during annealing and post annealing modes in the 300–400 K range. At room temperature, an almost ideal behaviour is observed. We observe that whilst the ideality factor during annealing has an increasing trend, in the post annealing mode, it has a decreasing trend with increase in temperature. A similar increase in barrier height with temperature in the post annealing mode has been observed in Au/n-Si Schottky diodes and was explained in terms of metallic-like phases produced on the interface because of the annealing process [22]. This change in post annealing characteristics is of a low order of magnitude as shown in Fig. 3 by a nominally flat post annealing curve. However, the change may be due to degradation of diode characteristics since the ideality factor is increasing. Whilst the measurements during annealing show an improvement in the diode's characteristics, post annealing measurements show that the diodes become poorer with increasing annealing temperatures above 400 K.

According to the Schottky-Mott theory, depletion layer capacitance can be expressed as [29]:

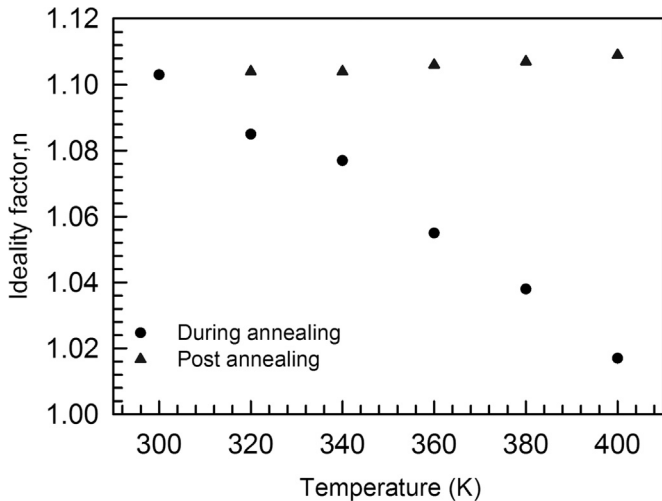


Fig. 3. Plots of ideality factor, n versus temperature during and post annealing.

$$C^{-2} = \frac{2(V_{bi} - V_A)}{q\epsilon_s A^2 N_D} \quad (4)$$

where, A is the diode area, V_{bi} the diffusion potential at zero bias obtained from the extrapolation of the linear C^{-2} - V plot to the V axis; and, V_A is the applied voltage. The capacitance of a Schottky diode is characterised by the width of the depletion layer [30]. The intercept on the voltage axis gives the diffusion potential V_{bi} which is used to determine the barrier height [24]:

$$\phi_{CV} = V_{bi} + V_0 \quad (5)$$

where V_0 is the potential difference between the conduction band minima and the Fermi level in the neutral part of the semiconductor [31], and is given by:

$$V_0 = kT \ln\left(\frac{N_C}{N_D}\right) \quad (6)$$

where N_C is density of states in the conduction band and N_D the free carrier concentration obtained from the gradient of the C^{-2} - V plots. From our results, all the C^{-2} - V plots were straight lines. ϕ_{CV} is observed to be higher than the ϕ_{IV} in all cases at all temperatures. Werner and Güttler [32] ascertained that spatial variations in the barriers cause current to flow preferentially through band minima causing I - V barrier height to be lower. The disparity can also be a result of the existence of “excess” capacitance [12].

The values of ϕ_{CV} during annealing show a general decrease across the 80–480 K range. This temperature dependence has been explained using the potential fluctuations model [32] as due to Schottky barrier height inhomogeneities. Fig. 4 shows a comparison of ϕ_{CV} post and during annealing. The post annealing values are overall lower, at all temperatures. The observed ϕ_{CV} trend during annealing shows a change in the temperature slope around 400 K. We fitted the C - V barrier height curve into two linear regions as shown in Fig. 5. The 300–400 K and 400–480 K regions yield equations of the form [24]: $\phi_{b(T1-T2)} = \phi(T=0) + \alpha T$ where α is the temperature coefficient in the given temperature range $T1$ – $T2$. The linear fitting results in two equations:

$$\phi_{b300-400 K} = -2.19 \times 10^{-4}T + 1.06 \text{ eV} \quad (7)$$

$$\phi_{b400-480 K} = -6.90 \times 10^{-4}T + 1.25 \text{ eV} \quad (8)$$

We propose that the sharp increase in carrier concentration within the 340–400 K range, as shown in Fig. 5, could be explained by the EL2 defect which we observed using L-DLTS measurements. The EL2 deep donor as shown in Fig. 6(inset) is located at an

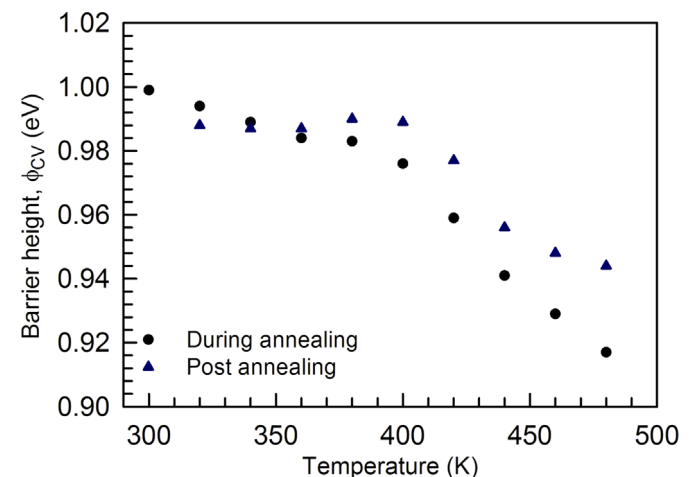


Fig. 4. Plots of C - V barrier height, ϕ_{CV} versus temperature during and post annealing.

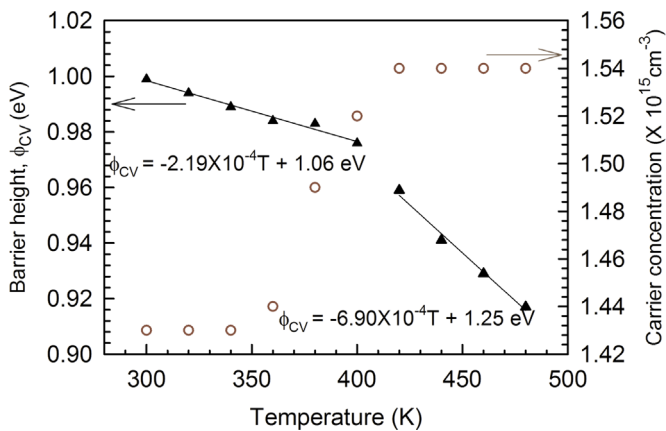


Fig. 5. Free carrier concentration and C–V barrier height, ϕ_{CV} versus temperature during annealing.

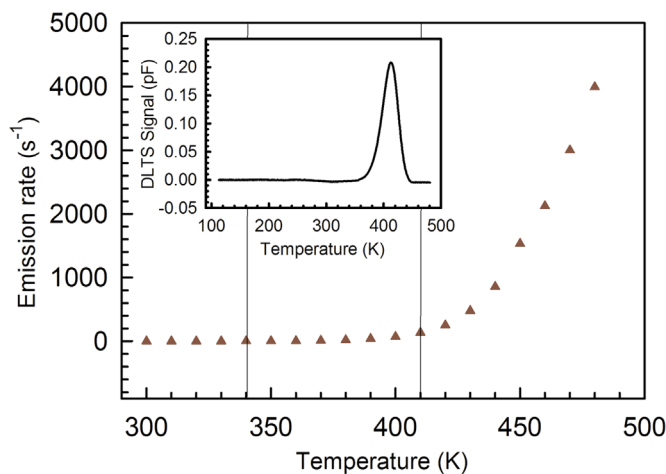


Fig. 6. Emission rate of the EL2 defect as a function of temperature. Inset: DLTS signal for as deposited diodes measured at a reverse bias of -2 V, a filling pulse $V_p = 0$ V and at a rate window of 80 s $^{-1}$.

energy level of 0.83 eV below the conduction band minima and has an apparent capture cross section of 2.4×10^{-13} cm 2 .

The atomistic origin of this defect has been a subject of controversy for several decades but it is widely believed to involve an arsenic antisite [33]. Fig. 6 shows the emission rate of the EL2 as a function of temperature. The graph is divided into three grid sections. In the 300 – 340 K temperature range there is not enough energy to release free carriers from the traps, the carrier concentration (Fig. 5) remains nominally constant and it is consistent with the emission rate (Fig. 6) in the same temperature range which is relatively flat. The increasing annealing temperature in the 340 – 400 K range causes the EL2 to release trapped charges, thus increasing the free carrier density (Fig. 5) [24]. There is a correlation with the increase in the emission rate of the EL2 in the same temperature range. This is also supported by the nominally flat post-annealing ϕ_{CV} and that during annealing, the ϕ_{CV} is characterised by a low temperature coefficient below 400 K. Since the ϕ_{CV} is determined from the charge balance details between the metal, the interface and the semiconductor, it will change to maintain this balance [17].

Above 400 K however, there is modification of the C–V Schottky barrier. The post annealing ϕ_{CV} is no longer flat, that is, it returns a “new” barrier height for each annealing. The barriers in both modes are now characterised by new temperature coefficients. This, we attribute to interfacial reactions at the interface between the gold and GaAs. Above 400 K, carrier concentration saturates, the reason being that the traps have released all the trapped free

carriers owing to the higher emission rate shown in Fig. 6.

However for the post-annealing mode, the carrier concentration saturates at a value lower than that for the annealing mode. The reasons for this are the subject of our current investigations. Besides the EL2, no other electrically active defects were observed by DLTS in the as received samples.

4. Conclusion

We have investigated the I – V and C – V characteristics of Au/n-GaAs Schottky diodes in the 80 – 480 K range. The ideality factor and ϕ_{IV} both modify permanently during annealing above 400 K. The post annealing results also show that diodes exposed to higher temperatures modify permanently. C – V measurements show a general decrease in ϕ_{CV} both during and post annealing. Our results suggest that exposure of the Au/n-GaAs Schottky barrier diodes to high temperatures above 400 K lead to their physical modification. We also observed an abrupt rise in the free carrier concentration about 340 – 400 K which we attributed to the emissions of trapped charges by the EL2 defect.

Acknowledgement

The authors gratefully acknowledge financial assistance from the University of Pretoria, the South African National Research Foundation grant#88021 and Johan Janse van Rensburg for technical assistance.

References

- [1] R.H. van Leest, G.J. Bauhuis, P. Mulder, R. van der Heijden, E. Bongers, E. Vlieg, J. J. Schermer, Effects of copper diffusion in gallium arsenide solar cells for space applications, *Solar Energy Mater. Solar Cells* 140 (2015) 45–53.
- [2] R.A. Pucel, H.A. Haus, H. Statz, Signal and noise properties of gallium arsenide microwave field-effect transistors, in: L. Marton (Ed.), *Advances in Electronics and Electron Physics*, Academic Press, New York, 1975, pp. 195–265.
- [3] P. Werle, F. Slemr, K. Maurer, R. Kormann, R. Mücke, B. Jänker, Near- and mid-infrared laser-optical sensors for gas analysis, *Opt. Lasers Eng.* 37 (2002) 101–114.
- [4] M. Mamor, K. Bouziane, A. Tirbiyine, H. Alhamrashdi, On the electrical characteristics of Au/n-type GaAs Schottky diode, *Superlattices Microstruct.* 72 (2014) 344–351.
- [5] S. Hofling, M. Lerner, J. Beetz, T.B. Hoang, J.P. Sprengers, A. Gaggero, D. Sahin, L. Midolo, M. Skacel, L. Balet, P. Jiang, S. Jahanmirinejad, G. Frucci, N. Chauvin, F. Mattioli, R. Sanjines, R. Leoni, E. Engin, M.G. Thompson, J.L. O'Brien, A. Fiore, M. Kamp, Quantum integrated photonics on GaAs, in: *Conference on Optoelectronic and Microelectronic Materials & Devices (COMMAD)*, 2012, pp. 3–4.
- [6] C.K. Chia, A. Sridhara, M. Suryana, J.R. Dong, B.Z. Wang, G.K. Dalapati, D.Z. Chi, GaAs-Ge materials integration for electronic and photonic applications, In: *Proceedings of the 5th IEEE International Conference on Group IV Photonics*, 2008, pp. 294–296.
- [7] S.K.K. M.K. Hudait, Doping Dependence of the barrier height and ideality factor of Au/n-GaAs Schottky diodes at low temperature, *Phys. B: Condens. Matter* 307 (2001) 125–137.
- [8] E. Özavcı, S. Demirezen, U. Aydemir, Ş. Altındal, A detailed study on current-voltage characteristics of Au/n-GaAs in wide temperature range, *Sens. Actuators A: Phys.* 194 (2013) 259–268.
- [9] R.T. Tung, The physics and chemistry of the Schottky barrier height, *Appl. Phys. Rev.* 1 (2014) 011304.
- [10] R.T. Tung, Recent advances in schottky barrier concepts, *Mater. Sci. Eng.: R* 35 (2001) 1–138.
- [11] Ş. Karataş, Ş. Altındal, Analysis of I – V characteristics on Au/n-type GaAs Schottky structures in wide temperature range, *Mater. Sci. Eng.: B* 122 (2005) 133–139.
- [12] H. Özerli, İ. Karteri, Ş. Karataş, Ş. Altındal, The current–voltage and capacitance–voltage characteristics at high temperatures of Au Schottky contact to n-type GaAs, *Mater. Res. Bull.* 53 (2014) 211–217.
- [13] D. Korucu, A. Turut, H. Efeoglu, Temperature dependent I – V characteristics of an Au/n-GaAs Schottky diode analyzed using Tung’s model, *Phys. B: Condens. Matter* 414 (2013) 35–41.
- [14] D.M. Kim, D.H. Kim, S.Y. Lee, Characterization and modeling of temperature-dependent barrier heights and ideality factors in GaAs Schottky diodes, *Solid-*

- State Electron. 51 (2007) 865–869.
- [15] E. Gür, S. Tüzemen, B. Kiliç, C. Coşkun, High-temperature Schottky diode characteristics of bulk ZnO, *J. Phys.: Condens. Matter* 19 (2007) 196206.
 - [16] Z. Xiaoling, L. Fei, L. Changzhi, X. Xuesong, L. Ying, M.S. N, High-temperature characteristics of Al_xGa_{1-x}N/GaN Schottky diodes, *J. Semicond.* 30 (2009) 034001.
 - [17] S.M. Sze, *Physics of semiconductor devices*, 2nd ed., Wiley (1981), p. 250–300.
 - [18] F. Auret, D. M. G, Annealing characteristics and thermal stability of electron beam evaporated Schottky contacts on GaAs, *Appl. Phys. Lett.* 60 (1992) 604.
 - [19] R.E. Miles, P.J. Tasker, D.V. Morgan, M.J. Howes, Schottky contacts on annealed GaAs, *Thin Solid Films* 104 (1983) 319–326.
 - [20] G. Myburg, W.O. Banard, W.E. Meyer, F. Auret, D., H. Burger, Vacuum annealing characteristics of electron beam evaporated Ruthenium contacts to n-GaAs grown by organometallic vapour epitaxy thin films, *Thin Solid Films* 213 (1992) 113–116.
 - [21] H. Sharda, K. Prasad, L. Faraone, A.G. Nassibian, Annealing studies on Pd/n-GaAs Schottky diodes, *Semicond. Sci. Technol.* 6 (1991) 765–770.
 - [22] Ç. Nuhoğlu, Y. Gülen, The effect of high temperature annealing on Schottky diode characteristics of Au/n-Si contacts, *Vacuum* 84 (2010) 812–816.
 - [23] M.A. Mayimele, M. Diale, W. Mtangi, F.D. Auret, Temperature-dependent current–voltage characteristics of Pd/ZnO Schottky barrier diodes and the determination of the Richardson constant, *Mater. Sci. Semicond. Process.* 34 (2015) 359–364.
 - [24] W. Mtangi, F.D. Auret, C. Nyamhere, P.J. Janse van Rensburg, A. Chawanda, M. Diale, J.M. Nel, W.E. Meyer, The dependence of barrier height on temperature for Pd Schottky contacts on ZnO, *Phys. B: Condens. Matter* 404 (2009) 4402–4405.
 - [25] R.F. Schmitsdorf, T.U. Kampen, W. Mönch, Explanation of the linear correlation between barrier heights and ideality factors of real metal-semiconductor contacts by laterally nonuniform Schottky barriers, *J. Vac. Sci. Technol. B* 15 (1997) 1221–1226.
 - [26] R.T. Tung, Electron transport at metal-semiconductor interfaces: general theory, *Phys. Review B* 45 (1992) 13509–13523.
 - [27] V. Janardhanam, Y.-K. Park, K.-S. Ahn, C.-J. Choi, Carrier transport mechanism of Se/n-type Si Schottky diodes, *J. Alloy. Compd.* 534 (2012) 37–41.
 - [28] R. Sharma, Temperature Dependence of I–V Characteristics of Au/n-Si Schottky barrier diode, *J. Electron. Dev.* 8 (2010) 286–292.
 - [29] M. Diale, F.D. Auret, Effects of chemical treatment on barrier height and ideality factors of Au/GaN Schottky diodes, *Phys. B: Condens. Matter* 404 (2009) 4415–4418.
 - [30] A. Sharma, P. Kumar, B. Singh, S.R. Chaudhuri, S. Ghosh, Capacitance-voltage characteristics of organic Schottky diode with and without deep traps, *Appl. Phys. Lett.* 99 (2011) 023301.
 - [31] Ş. Karataş, Ş. Altındal, Temperature dependence of barrier heights of Au/n-type GaAs Schottky diodes, *Solid-State Electron.* 49 (2005) 1052–1054.
 - [32] J.H. Werner, H.H. Güttler, Barrier inhomogeneities at Schottky contacts, *J. Appl. Phys.* 69 (1991) 1522–1533.
 - [33] M. Kaminska, E.R. Weber, EL2 defect in GaAs, in: R.W. Eicke (Ed.), *Semiconductors and Semimetals*, Elsevier, Amsterdam, 1993, pp. 59–89.